Signal propagation in electron waveguides: Transmission-line analogies

Jan-Olof J. Wesström
The Laboratory of Photonics and Microwave Engineering, Department of Electronics, Royal Institute of Technology, Electrum 229, S-164 40 Kista, Sweden
(Received 20 November 1995)

Signal propagation along an electron waveguide with a nearby screening metal plane is investigated. It is mediated by one-dimensional intrasubband plasma oscillations or space-charge waves. The signals therefore propagate much slower than the velocity of light. A transmission-line model and a characteristic impedance are theoretically derived. Discontinuities (changing width of an electron waveguide, junction to a bulk conductor, and elastic electron scatterer) are modeled as changes in characteristic impedance and insertions of equivalent series elements. In the limit of short waveguide sections, the two versions of the Landauer formula for conductance $G=G_0T$ and $G=G_0T/(1-T)$ are obtained. In the limit of many subbands, the velocity of light is reached. [S0163-1829(96)03540-0]

I. INTRODUCTION

Recent development in semiconductor processing has made it possible to fabricate structures with dimensions comparable to the electron wavelength, in particular electron waveguides. Several switches based on the one-dimensional (1D) nature of electron gases in these thin semiconductor wires have been suggested. Some examples of these electron waveguide devices are Aharonov-Bohm interferometers,[1] directional couplers,[2] the quantum stub transistor,[3] and the Y-branch switch.[4]

These devices are thought of as one possibility of approaching terahertz switching frequencies.[5] When cascading at high frequencies, the delay due to signal propagation has to be considered. Since the devices are based on electron waveguides, the first part of the leads from their source and drain will necessarily be formed by electron waveguides. Often, the cross-section geometry around an electron waveguide is similar to the geometry of a microstrip transmission line: a conductor (the electron waveguide) close to a conducting plane (Fig. 1). In the split gate configuration,[6] for example, the conducting plane consists of the gate metal. Although the cross section is very similar to the microstrip, the propagating modes are very different. At the bulk conductor of a microstrip the boundary condition of vanishing longitudinal electric field at the conductor yields a TEM mode (if all dielectrics surrounding the conductor have the same dielectric constant), propagating close to the speed of light.

In contrast, at an electron waveguide, although this also is a conductor, the field does not vanish. This is due to the ''quantum inductance'' related to the inertia of the electrons. The phenomenon appears when the 1D density of free charges is drastically reduced, as in a 1D structure. Many authors have described the resulting intrasubband plasmons, their dispersion relations, and their interaction with light, using, for example, the random-phase approximation[7] or a hydrodynamic theory.[8] This article instead focuses on signal propagation, important in cascading of electron waveguide devices. It develops a transmission-line model including equivalent characteristic impedances and scattering matrices for different kinds of junctions. It might be seen as an attempt to extend the linear-response theory into the high-frequency regime. To simplify, the action of the electromagnetic forces on the electrons is analyzed with classical mechanics. The only quantum-mechanical effect considered is density of states and the Pauli exclusion principle. It turns out that signals in these plasma waveguides, as they will be called here, have a velocity hundreds of times slower and a characteristic impedance hundreds of times higher compared to the corresponding values of a TEM waveguide formed only by macroscopic conductors.

II. SINGLE-MODE WAVE PROPAGATION

Let us consider an electron waveguide without any scattering under a perfectly conducting plane (Fig. 1). We will restrict ourselves to the case where the wavelength of the electron is much shorter than the signal wavelength, so the electron motion can be analyzed classically. Expressed in the

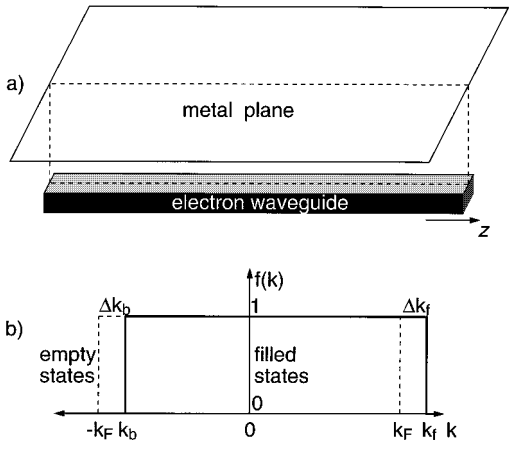

FIG. 1. (a) 1D plasma waveguide formed by an electron waveguide under an infinite conducting metal plane. (b) Population probability of the states as a function of k vector at a given time and point. At $T=0$ K all states between k_b and k_f are filled. All other states are empty. Δk_b and Δk_f are deviations from the equilibrium Fermi level k_F.

quantum-mechanical wave vector, Newton's equation of motion can be written

$$dk=\frac{F}{\hbar}dt, \tag{1}$$

where t is the time, k the wave vector of the electron, and F is the force applied to the electron by the electromagnetic field. Now let $k(t,z)$ be a function of time and a coordinate z along the electron waveguide. Differentiating, we obtain

$$dk=\frac{\partial k}{\partial t}dt+\frac{\partial k}{\partial z}dz. \tag{2}$$

Combining (1) and (2) we get

$$\frac{\partial k}{\partial t}=\frac{F}{\hbar}-\frac{dz}{dt}\frac{\partial k}{\partial z}=\frac{F}{\hbar}-\frac{\hbar k}{m}\frac{\partial k}{\partial z}, \tag{3}$$

where $\hbar k/m$ is the velocity of the electron and m is its effective mass.

The above equation can easily be used to relate variations in charge and current in a degenerately populated 1D subband. When the temperature is $T=0$K all backward traveling states with $k>k_b$ and all forward traveling states with $k<k_f$ are filled with electrons and all other states are empty as in Fig. 1. Then the charge per unit length ρ and current I in the electron waveguide are

$$\rho=-\frac{q}{\pi}(k_f-k_b) \tag{4}$$

and

$$I=-\frac{\hbar}{2m}\frac{q}{\pi}(k_f^2-k_b^2). \tag{5}$$

The electron charge is denoted $-q$. Assuming small variations around the Fermi level k_F as in Fig. 1,

$$\Delta k_f=k_f-k_F,\ \ \Delta k_b=k_b+k_F, \tag{6}$$

the deviations in charge is

$$\Delta\rho=\rho-\rho_0=-\frac{q}{\pi}(\Delta k_f-\Delta k_b), \tag{7}$$

where

$$\rho_0=-\frac{q}{\pi}2k_F \tag{8}$$

is the equilibrium charge. The small signal current expressed in Δk_f and Δk_b is

$$I\approx-\frac{\hbar k_F}{m}\frac{q}{\pi}(\Delta k_f+\Delta k_b). \tag{9}$$

To get a relation between $\Delta\rho$ and I we apply (3) to k_b and k_f. For their difference and sum, (3) yields

$$\frac{\partial(k_f-k_b)}{\partial t}=-\frac{\hbar}{m}\left(k_f\frac{\partial k_f}{\partial z}-k_b\frac{\partial k_b}{\partial z}\right), \tag{10}$$

$$\frac{\partial(k_f+k_b)}{\partial t}=\frac{2F}{\hbar}-\frac{\hbar}{m}\left(k_f\frac{\partial k_f}{\partial z}+k_b\frac{\partial k_b}{\partial z}\right). \tag{11}$$

Using the expressions (6), (7), and (9) for deviations, (10) and (11) can be expressed in charge and current

$$\frac{\partial\Delta\rho}{\partial t}=-\frac{\partial I}{\partial z}, \tag{12}$$

$$\frac{\partial I}{\partial t}=-\frac{2v_F}{R_0}\frac{F}{q}-v_F^2\frac{\partial\Delta\rho}{\partial z}, \tag{13}$$

where we have used the expressions for the Fermi velocity and the resistance of a single-mode quantum point contact

$$v_F=\frac{\hbar k_F}{m},\ \ R_0=\frac{\hbar\pi}{q^2}\approx 13\ \text{k}\Omega. \tag{14}$$

Equation (12) is the equation of continuity and (13) is equivalent to the phenomenological equation of motion (6) in the hydrodynamic approach of Mendoza and Schaich.[8] However, there the parameter corresponding to v_F^2 was obtained by fitting the dispersion to that of the random-phase approximation. It is interesting to note that in absence of electromagnetic forces $F=0$, a signal would propagate with a velocity of $u=v_F$ according to (12) and (13), as expected.

Maxwell's equations can be used to calculate the electromagnetic force F, given a cross-section geometry and charge and current distributions. If the distance to the metal plane is larger than the wavelength of the plasma wave or if there is no such plane, as in an etched and epitaxially overgrown electron waveguide,[9] the force will depend heavily on the wavelength. To simplify, let us now assume that the charge and current vary slowly with z so that this is not the case. Then, the force $F(t,z)$ can be calculated locally from $\Delta\rho(t,z)$ and $I(t,z)$:

$$F=-qE_z=q\left(\frac{\partial V}{\partial z}+\frac{\partial A_z}{\partial t}\right)=\frac{q}{C_g}\frac{\partial\Delta\rho}{\partial z}+qL_g\frac{\partial I}{\partial t}, \tag{15}$$

where E_z is the longitudinal component of the electric field in the electron waveguide. V and A are the electric and magnetic potentials. C_g and L_g, defined in (15), are the capacitance and inductance per unit length for the given geometry. If we insert the expression for the force on the electron (15) into (13) and rearrange we get

$$\left(L_g+\frac{R_0}{2v_F}\right)\frac{\partial I}{\partial t}=-\left(\frac{1}{C_g}+\frac{R_0v_F}{2}\right)\frac{\partial\Delta\rho}{\partial z}. \tag{16}$$

The corresponding equation for a TEM waveguide is

$$L\frac{\partial I}{\partial t}=-\frac{1}{C}\frac{\partial\Delta\rho}{\partial z}. \tag{17}$$

One could say that the inductance and capacitance have been modified by the reduced density of states

$$L_{\text{tot}}=L_g+\frac{R_0}{2v_F},\ \ \frac{1}{C_{\text{tot}}}=\frac{1}{C_g}+\frac{R_0v_F}{2}. \tag{18}$$

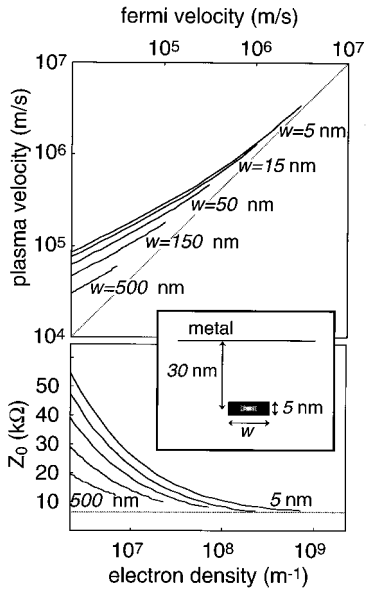

FIG. 2. Plasma wave velocity u and characteristic impedance Z_0 [Eqs. (22) and (27)] for an $In_{0.53}Ga_{0.47}As$ electron waveguide buried in InP as in the inset drawing. The curves are discontinued where the electron density (proportional to Fermi velocity v_F) is so high that it populates the second subband. u is always larger than v_F and Z_0 is always larger than $R_0/2$ (dashed lines).

The modification of L is related to the mass inertia of the electrons. C_{tot} is the electrochemical capacitance[10] per unit length defined as

$$\frac{1}{C_{\text{tot}}} = -\frac{1}{q}\frac{d\mu}{d\rho}, \tag{19}$$

where μ is the electrochemical potential. This is easily shown using (8) and (14):

$$-\frac{1}{q}\frac{d\mu}{d\rho} = -\frac{1}{q}\left(\frac{d(-qV)}{d\rho} + \frac{dE_F}{dk_F}\frac{dk_F}{d\rho}\right) = \frac{1}{C_g} + \frac{\hbar^2 k_F}{m}\frac{\pi}{2q^2} = \frac{1}{C_g} + \frac{R_0 v_F}{2}, \tag{20}$$

where V is the electrostatic potential, E_F is the Fermi energy, and C_g is the electrostatic (conventional) capacitance

$$\frac{1}{C_g} = \frac{dV}{d\rho}. \tag{21}$$

Solving the telegraph equations (16) and (12) for propagation velocity, using (18) we get

$$u = \sqrt{\frac{1}{L_{\text{tot}}C_{\text{tot}}}} = \sqrt{\frac{\frac{1}{C_g} + \frac{R_0 v_F}{2}}{L_g + \frac{R_0}{2v_F}}}. \tag{22}$$

This equation is illustrated in Fig. 2. C_g was calculated for a rectangular $In_{0.53}Ga_{0.47}As$ electron waveguide buried in InP, assuming cosine-shaped electron wave functions. The cross-section geometry is seen in the inset figure. L_g was neglected since it is much smaller than $R_0/2v_F$. Note that these velocities are orders of magnitude lower than the velocity for the corresponding TEM wave in a waveguide formed by bulk conductors $u_B = c/\sqrt{\epsilon_r} \approx 8.5\times 10^7$ m/s. As seen in the figure, u is, however, always larger than the Fermi velocity. Even for these quite low velocities, the assumption of a wavelength much longer than the distance to the metal plane is valid up into the terahertz region, yielding low dispersion in this frequency range.

The most natural way to increase the propagation velocity is to decrease the dimensions of the electron waveguide. A thinner electron waveguide yields lower C_g and gives larger subband separation, which allows a higher v_F (proportional to electron density) in an electron waveguide before the second subband is populated. Another way to decrease C_g is to increase the distance to the metal plane. The velocity is, however, still quite low, so to further decrease signal delays between cascaded electron waveguide devices one has to couple the signal to a conventional electromagnetic waveguide. Therefore, it is crucial to study the reflection and transmission at discontinuities.

Before we derive the scattering matrices for three different types of junctions we will derive the relations between a few important variables: current, charge, and voltage. First, we let these quantities have exponential temporal and spatial dependence $e^{j(\omega t \mp \beta z)}$, where the upper (lower) sign, as in the following, corresponds to waves traveling in the positive (negative) z direction. The equation of continuity (12) then yields

$$I = \pm\frac{\omega}{\beta}\Delta\rho = \pm u\Delta\rho. \tag{23}$$

The electrostatic voltage can be related to the charge using $\Delta V = \Delta\rho/C_g$. For an electron waveguide, however, μ is a more natural variable than V. Let us therefore define a convenient ''electrochemical voltage''

$$\Delta W = -\frac{1}{q}\Delta\mu = \frac{\Delta\rho}{C_{\text{tot}}}. \tag{24}$$

At the last equality, (19) was used. It can be shown, in a straightforward but mathematically lengthy way, that the energy transport is $P = I\Delta W$ if both the kinetic energy of the electrons and the electromagnetic energy is included. For a bulk conductor, where the density of states is high, $\Delta\mu = -q\Delta V$ so that

$$\Delta W_B = \Delta V_B. \tag{25}$$

These conditions make ΔW a suitable generalization of ΔV. Dividing (24) by (23) we get

$$\frac{\Delta W}{I} = \pm\frac{1}{uC_{\text{tot}}} = \pm Z_0, \tag{26}$$

where Z_0 is the equivalent characteristic impedance

$$Z_0 = \frac{1}{uC_{\text{tot}}} = \sqrt{\frac{L_{\text{tot}}}{C_{\text{tot}}}}. \tag{27}$$

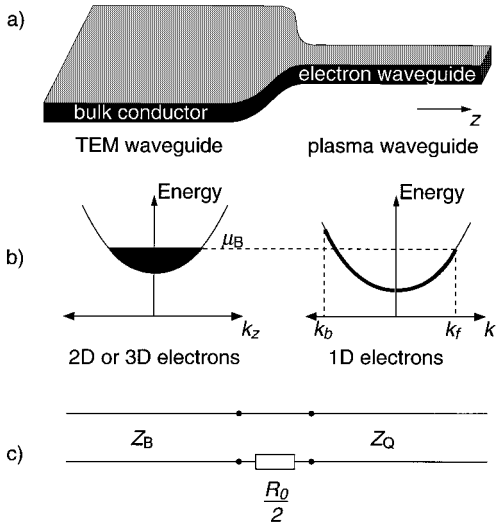

FIG. 3. (a) Junction between a TEM waveguide formed by a bulk conductor on the left-hand side and a 1D plasma waveguide formed by an electron waveguide on the right-hand side. (b) In the end of the bulk conductor an electrochemical potential μ_B is assumed. This level governs k_f in the first part of the electron waveguide. (c) The junction can be modeled by two transmission lines with different characteristic impedances and an inserted series resistance of $R_0/2$.

Note that this definition coincides with the conventional one for bulk waveguides since there $C_{\text{tot}}=C_g$ and $L_{\text{tot}}=L_g$. Z_0 is low for high Fermi velocities and wide electron waveguides, as can be seen in Fig. 2.

III. SCATTERING MATRIX FOR JUNCTION BETWEEN A TEM WAVEGUIDE AND A SINGLE-MODE PLASMA WAVEGUIDE

To model the interface between a TEM waveguide and a plasma waveguide, we assume that the end of the bulk conductor constitutes an electron reservoir with an electrochemical potential μ_B that governs k_f, the wave vector of the fastest electron injected into the electron waveguide (see Fig. 3). This is the situation if the electrons thermalize in the bulk conductor much before they have traveled one TEM wavelength in this conductor. This is likely since this wavelength is long due to the high velocity there. We also assume that the junction is adiabatic from an electron-wave point of view, i.e., the transmission coefficient of the electron injection is unity. These are the same assumptions as are generally used to derive conductance quantization.[11] Finally, we assume that the junction is sudden in comparison with the plasma wavelength. Thus the first boundary condition is

$$\mu_B=\frac{\hbar^2k_f^2}{2m}-q\left(\frac{\rho_Q}{C_g}+V_0\right), \tag{28}$$

where V_0 is the potential in the electron waveguide when the charge there ρ_Q is zero. The second boundary condition is current continuity

$$I_B=I_Q. \tag{29}$$

When only small signals are considered and (28) is divided by $-q$ the equation turns into

$$\Delta V_B=-\frac{\Delta\mu_B}{q}=-\frac{\hbar^2k_F}{qm}\Delta k_f+\frac{\Delta\rho_Q}{C_g}. \tag{30}$$

Δk_f can be expressed in current and charge using (7) and (9). Inserting the resulting expression in (30), we obtain

$$\Delta V_B=\frac{R_0}{2}I_Q+\left(\frac{R_0v_F}{2}+\frac{1}{C_g}\right)\Delta\rho_Q. \tag{31}$$

The parenthesis is $1/C_{\text{tot}}$ according to (18), and using (24) we get

$$\Delta V_B=\frac{R_0}{2}I_Q+\Delta W_Q, \tag{32}$$

which is the boundary condition (24) expressed in current and voltages.

To derive the scattering matrix, we first assume that a wave ΔV_B^+ impinges from the TEM waveguide on the left-hand side onto the electron waveguide, ΔV_B^- is reflected back, and ΔW_Q^- is transmitted. Using the boundary conditions (32) and (29) together with (26) with $Z_0=Z_B$ for the TEM waveguide and $Z_0=Z_Q$ for the electron waveguide remembering (25), one obtains the first two elements of the scattering matrix for the junction, S_{11} and S_{12}. In the same way, assuming the incident wave W_Q^+ coming from the plasma waveguide, one obtains the other two elements. The whole matrix becomes

$$S_{BQ}=\begin{pmatrix}\dfrac{Z_Q+R_0/2-Z_B}{Z_B+Z_Q+R_0/2} & \dfrac{2Z_B}{Z_B+Z_Q+R_0/2}\\ \dfrac{2Z_Q}{Z_B+Z_Q+R_0/2} & \dfrac{Z_B+R_0/2-Z_Q}{Z_B+Z_Q+R_0/2}\end{pmatrix}, \tag{33}$$

relating incident and outgoing waves

$$\begin{pmatrix}\Delta V_B^-\\ \Delta W_Q^-\end{pmatrix}=S_{BQ}\begin{pmatrix}\Delta V_B^+\\ \Delta W_Q^+\end{pmatrix}. \tag{34}$$

This is the same scattering matrix as in the junction between two conventional transmission lines with characteristic impedances Z_B and Z_Q with an inserted series resistance of $R_0/2\approx 6.5\ \text{k}\Omega$ as in Fig. 3. Note that in the limit of long wavelengths or short waveguide sections, this model yields the expected[12] total dc resistance of R_0 of an electron waveguide without scattering, as measured between the two reservoirs. The dissipation associated with the resistance is in accordance with the assumption of an electrochemical potential μ_B. The existence of μ_B implies that electrons from the electron waveguide are thermalized in the bulk conductor.

If we want to use ordinary waveguides for signaling between our electron waveguide devices, it is important to match the impedances to maximize transmission at the junctions. It is probably very difficult to transform the low impedance of the TEM waveguide (typically 50 Ω) to the high Z_Q (around 20 kΩ as in Fig. 2), but if this can be done the transmission to and from the plasma waveguide should be good, especially if $Z_Q \gg R_0/2$ so that there is little dissipation. If impedance matching is not possible it will be necessary to

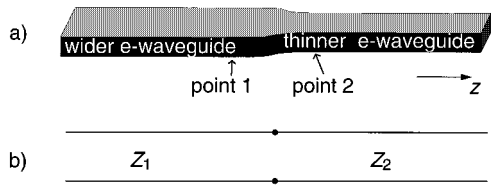

FIG. 4. (a) Junction between two 1D plasma waveguides formed by electron waveguides with different widths. (b) The junction can be modeled by a transmission-line equivalent consisting of two sections with different characteristic impedances.

make the electron waveguide sections much shorter than the plasma wavelength and the ordinary conductors much shorter than the wavelength there. Then reflections cancel and all components can be thought of as lumped. For extremely high frequencies this is not possible either. Then, cascading will be impossible since less than 1% of the power is transmitted to a plasma waveguide, if $Z_B=50\ \Omega$. The ''optimum'' is achieved when the plasma waveguide has a characteristic impedance around $R_0/2$. This is the case when $C_g \gg 2/(R_0 v_F)$.

IV. SCATTERING MATRIX FOR JUNCTIONS BETWEEN DIFFERENT SINGLE-MODE PLASMA WAVEGUIDES

Another type of discontinuity is between two sections of plasma waveguides with different geometries causing differences in v_F and C_g and therefore also in $C_{\rm tot}$ and Z_0. See Fig. 4. To calculate the scattering matrix for this case we assume that the transition region is much shorter than the plasma wavelength, but much longer than the electron wavelength, so that there are no electron reflections. The first boundary condition is current continuity

$$I_1=I_2. \tag{35}$$

Since the electrons are not scattered, it is also natural to assume the electrochemical potential to be continuous,

$$\Delta W_1=\Delta W_2. \tag{36}$$

These boundary conditions are analogous to those of a junction between two waveguide sections in transmission-line theory, where the current and voltage are continuous. See Fig. 4. These conditions yield a scattering matrix

$$S_{QQ}=\begin{pmatrix} \dfrac{Z_2-Z_1}{Z_1+Z_2} & \dfrac{2Z_1}{Z_1+Z_2} \\ \dfrac{2Z_2}{Z_1+Z_2} & \dfrac{Z_1-Z_2}{Z_1+Z_2} \end{pmatrix}. \tag{37}$$

The validity of (36) must, however, be examined. Assuming a constant effective mass, but allowing a z dependence for the voltage in the absence of electrons $V_0(z)$ and for $C_g(z)$ and $L_g(z)$, (15) is modified

$$F=q\left(\frac{\partial V}{\partial z}+\frac{\partial A_z}{\partial t}\right)=q\frac{\partial}{\partial z}\left(V_0(z)+\frac{\rho_0(z)+\Delta\rho(z)}{C_g(z)}\right)+qL_g(z)\frac{\partial I}{\partial t}. \tag{38}$$

The equilibrium of the electrochemical potential

$$\mu_0=-q\left(V_0+\frac{\rho_0}{C_g}\right)+\frac{\hbar^2k_F^2}{2m} \tag{39}$$

has to be constant along the electron waveguide. This can be used in (38) to eliminate V_0 and ρ_0. The resulting expression for the force is inserted into (11) and we get

$$\frac{\partial(k_f+k_b)}{\partial t}=\frac{2}{\hbar}\left[\frac{\partial}{\partial z}\left(q\frac{\Delta\rho}{C_g}+\frac{\hbar^2k_F^2}{2m}\right)+qL_g\frac{\partial I}{\partial t}\right]-\frac{\hbar}{m}\left(k_f\frac{\partial k_f}{\partial z}+k_b\frac{\partial k_b}{\partial z}\right). \tag{40}$$

Using (9), (14), and (18) we can write this as

$$-L_{\rm tot}\frac{\partial}{\partial t}I=\frac{\partial}{\partial z}\left(\frac{\Delta\rho}{C_g(z)}-\frac{\hbar^2}{4qm}(k_f^2-k_F^2+k_b^2-k_F^2)\right). \tag{41}$$

Integrating this from point 1 to point 2 and applying (6), (7), and (18) we get

$$-\frac{\partial}{\partial t}\int_1^2 L_{\rm tot}I\,dz=\frac{\Delta\rho_2}{C_{\rm tot,2}}-\frac{\Delta\rho_1}{C_{\rm tot,1}}. \tag{42}$$

The right-hand side is a difference between electrochemical voltages, so if the left-hand side can be shown to be small, (36) is verified. Taking the absolute value of (42) at a specific frequency, we get

$$|\Delta W_2-\Delta W_1|\leqslant\left|\int_1^2\omega L_{\rm tot}(z)\frac{\Delta W(z)}{Z_0(z)}dz\right|=\left|\int_1^2\omega\frac{\Delta W(z)}{u(z)}dz\right|=\left|\int_1^2\frac{2\pi}{\lambda(z)}\Delta W(z)dz\right|, \tag{43}$$

where (26) and (27) have been used. Equation (43) implies that (36) is a good approximation as long as the transition region is much shorter than the plasma wavelength, and for this case the scattering matrix (37) is verified.

V. SCATTERING MATRIX FOR PLASMA WAVE AT ELECTRON REFLECTION SITE IN A SINGLE-MODE PLASMA WAVEGUIDE

A third kind of discontinuity is depicted in Fig. 5. It occurs in a plasma waveguide where there is some kind of imperfection, reflecting the electrons with a probability R_e. In the reflection and transmission the electrons conserve their energy, i.e., the electrons impinging on the imperfection from electron waveguide 1, having wave vectors $0<k<k_{f1}$ are reflected with a probability R_e into left going states $-k_{f1}<k<0$. In transmissions, however, the momentum is not conserved since there is a difference in electrostatic potential caused by charge differences. Instead, the electrons

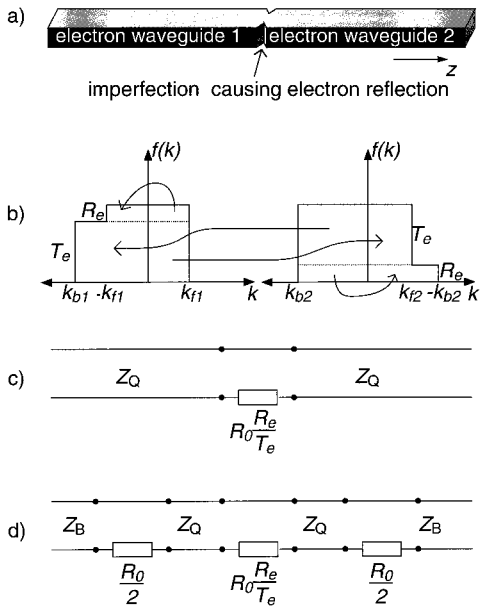

FIG. 5. (a) 1D plasma waveguide formed by an electron waveguide with imperfection causing an electron reflection. (b) Population probability of the states as a function of k vector on both sides of the junction. The forward traveling states on the left-hand side have $k<k_{f1}$. These electrons are reflected into backward traveling states $k>-k_{f1}$ with a probability R_e. The other part of the population probability of the backward traveling states is formed by transmission from the right-hand side. The corresponding diagram on the right-hand side can be drawn after analogous contemplations. (c) The imperfection can be modeled by a transmission line with an inserted series resistance of R_0R_e/T_e. (d) Transmission-line equivalent of the electron waveguide with imperfection between bulk conductors.

are transmitted with a probability $T_e=1-R_e$ into states with $k<k_{f2}$, where k_{f2} can be determined by energy conservation

$$\frac{\hbar^2k_{f2}^2}{2m}-q\frac{\rho_2}{C_g}=\frac{\hbar^2k_{f1}^2}{2m}-q\frac{\rho_1}{C_g}. \tag{44}$$

Using small signal analysis (6) and (7), assuming that the steady states are the same on both sides we get

$$\Delta k_{f2}-\Delta k_{f1}=+\frac{q}{\hbar v_F}\frac{\Delta\rho_2-\Delta\rho_1}{C_g} \tag{45}$$

and similarly for electrons from electron waveguide 2

$$\Delta k_{b2}-\Delta k_{b1}=-\frac{q}{\hbar v_F}\frac{\Delta\rho_2-\Delta\rho_1}{C_g}. \tag{46}$$

The charge for the electron distribution in Fig. 5 can be written in analogy with (7):

$$\Delta\rho_1=-\frac{q}{\pi}\{\Delta k_{f1}-[(1-R_e)\Delta k_{b1}-R_e\Delta k_{f1}]\}$$

$$=-\frac{q}{\pi}[(1+R_e)\Delta k_{f1}-(1-R_e)\Delta k_{b1}], \tag{47}$$

$$\Delta\rho_2=-\frac{q}{\pi}[(1-R_e)\Delta k_{f2}-R_e\Delta k_{b2}-\Delta k_{b2}]$$

$$=-\frac{q}{\pi}[(1-R_e)\Delta k_{f2}-(1+R_e)\Delta k_{b2}] \tag{48}$$

for the two sides of the discontinuity respectively. Using (45) and (46), we can eliminate Δk_{f2} and Δk_{b2} from (48). If we now subtract (47) from the resulting equation and simplify we get

$$\Delta\rho_2-\Delta\rho_1=-\frac{2q^2}{\pi C_g v_F\hbar}(\Delta\rho_2-\Delta\rho_1)$$

$$+2R_e\frac{q}{\pi}(\Delta k_{f1}+\Delta k_{b1}). \tag{49}$$

Here we can solve for $\Delta\rho_2-\Delta\rho_1$ and simplify using (14) and (18):

$$\Delta\rho_2-\Delta\rho_1=C_{\rm tot}R_0R_ev_F\frac{q}{\pi}(\Delta k_{f1}+\Delta k_{b1}). \tag{50}$$

The current through the discontinuity can be expressed as

$$I=-\frac{q}{\pi}v_F[(1-R_e)\Delta k_{b1}-R_e\Delta k_{f1}+\Delta k_{f1}]$$

$$=-\frac{q}{\pi}v_F(1-R_e)(\Delta k_{f1}+\Delta k_{b1}), \tag{51}$$

modifying (9) bearing Fig. 5 in mind. Combining (50) and (51) we get

$$\Delta\rho_2-\Delta\rho_1=-C_{\rm tot}\frac{R_e}{1-R_e}R_0I. \tag{52}$$

If we divide this by $C_{\rm tot}$ and use (24), we get

$$\Delta W_2-\Delta W_1=-R_sI, \tag{53}$$

where

$$R_s=\frac{R_e}{1-R_e}R_0=\frac{R_e}{T_e}R_0. \tag{54}$$

Now we have put the boundary condition in a convenient form. Together with current continuity as in (35) this is equivalent to the boundary condition at an inserted series resistance in a transmission line (see Fig. 5). This yields a scattering matrix

$$S_R=\begin{pmatrix}\frac{R_s}{2Z_Q+R_s} & \frac{2Z_Q}{2Z_Q+R_s}\\ \frac{2Z_Q}{2Z_Q+R_s} & \frac{R_s}{2Z_Q+R_s}\end{pmatrix}. \tag{55}$$

It is interesting to note that R_s is the same resistance as derived for a four-probe measurement (relating potential and current within the electron waveguide).[12] If we now put the electron waveguide with electron scatterer between two bulk conductors and combine its transmission-line model with our model for the two junctions to TEM waveguides (see Fig. 5), we may gain some insight into how R_s is related to the

resistance in a two-probe measurement. Since the three resistances are in series, the total resistance is

$$R_{\rm tot}=\frac{R_0}{2}+R_s+\frac{R_0}{2}=\frac{R_0}{T_e}, \tag{56}$$

which coincides with what we measure in a two-probe measurement.[12]

One practical implication of the derived scattering matrix is that plasma waveguides used to communicate between different devices should have high Z_Q (low C_g and v_F) in comparison with R_0, because then the plasma wave propagates well even where there is elastic scattering in the electron waveguide. This model should also be useful in designing quantum interference devices for high frequencies. A short Aharonov-Bohm interferometer could, for example, be modeled as an elastic scatterer. Z_Q should then be low so that the interferometer efficiently can impede an incoming plasma wave even if the electron reflection is not complete.

VI. MULTIMODE WAVE PROPAGATION

If there is more than one populated subband but no scattering between the subbands, (12) and (13) are still valid for each separate subband:

$$\frac{\partial\Delta\rho_m}{\partial t}=-\frac{\partial I_m}{\partial z}, \tag{57}$$

$$\frac{\partial I_m}{\partial t}=-\frac{2v_m}{R_0q}\sum_n F_{mn}-v_m^2\frac{\partial\Delta\rho_m}{\partial z}, \tag{58}$$

where ρ_m, I_m, v_m are the charge, current, and Fermi velocity of subband m and

$$F_{mn}=\frac{q}{C_{mn}}\frac{\partial\Delta\rho_n}{\partial z}+qL_{mn}\frac{\partial\Delta I_n}{\partial t} \tag{59}$$

is the force on the electrons in subband m caused by charge and current in subband n, which may depend on the indices since the wave functions have different extensions. These equations are useful to analyze the propagation in conductors of intermediate widths, which could, for example, form a transition between a bulk conductor and a single-mode electron waveguide in junctions similar to the one in Fig. 3. This kind of transition region could possibly help matching the impedance. The scattering matrix of such a junction is, however, beyond the scope of this article. Here we will only look at the signal propagation in these waveguides and show that for very many subbands (as in a bulk conductor) we obtain the velocity of light.

If the wave is periodic as $e^{j(\omega t-\beta z)}$ and we make the simplification that F_{mn}, $C_{mn}=C_g$, and $L_{mn}=L_g$ are the same for all combinations of indices, we can combine (57)–(59) into

$$\left(\frac{\omega^2}{\beta^2}-v_m^2\right)\frac{R_0C_g}{2v_m}I_m=\left(1-\frac{\omega^2}{\beta^2}C_gL_g\right)\sum_n I_n. \tag{60}$$

Using $u=\omega/\beta$ and $u_B=1/\sqrt{C_gL_g}$ we get

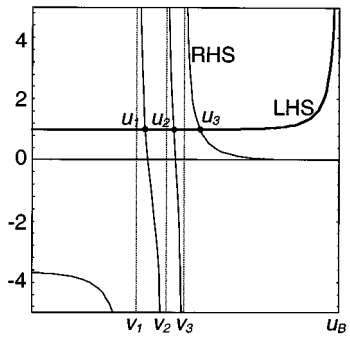

FIG. 6. Left- and right-hand sides of Eq. (63) for three populated subbands with Fermi velocities v_1, v_2, and v_3. The intersections give the velocities (u_1, u_2, and u_3) for the plasma modes. u_B is the propagation velocity for a bulk conductor. The velocity scale is logarithmic.

$$(u^2-v_m^2)\frac{R_0C_g}{2v_m}I_m=\left(1-\frac{u^2}{u_B^2}\right)\sum_n I_n. \tag{61}$$

The right-hand side is independent of the index m so the currents in two subbands l and m are related by

$$I_l=\frac{u^2-v_m^2}{u^2-v_l^2}\frac{v_l}{v_m}I_m. \tag{62}$$

This means that the direction of the current in a subband depends on whether the subband Fermi velocity is higher or lower than u. If (62) is inserted into the right-hand side of (61), we get

$$\frac{u_B^2}{u_B^2-u^2}=\frac{2}{R_0C_g}\sum_n\frac{v_n}{u^2-v_n^2}, \tag{63}$$

from which equation we can get the velocities u of the propagating modes. The equation is illustrated in Fig. 6. We see that there is one solution for u between each subband Fermi velocity v_n and that there is one solution with a higher velocity than all the Fermi velocities. When more subbands are added, the right-hand side of (63) increases for high u so that the fastest solution u_N moves toward u_B. Then $u\gg v_N$ and v_n^2 can be neglected on the right-hand side of (63). The velocity of the fastest mode is then given by

$$\frac{1}{u^2}\approx\frac{1}{u_B^2}+\frac{1}{\frac{2}{R_0C_g}\sum_n v_n}. \tag{64}$$

Here we see that for a bulk conductor (with very many subbands), $u\approx u_B$ as expected. To reach a velocity of $u=0.9u_B$, however, quite many subbands are needed. For a conductor with equal width and thickness at a distance from the metal plane six times the thickness of the conductor, we get $C_g\approx 200$ pF/m if the dielectric is InP. Then we need a sum of subband Fermi velocities of

$$\sum_n v_n\approx 5\times 10^{10}\ \text{m/s}. \tag{65}$$

This means that roughly 10^6 1D subbands in a semiconductor with $v_F\approx 10^5$ m/s are needed to reach this velocity. For a

gold wire where $v_F = 1.4 \times 10^6$ m/s, about 10^5 modes are needed, which is achieved when the cross-section area is $A \approx 10^{-15}$ m^2. This is a very small cross section, which explains why ordinary transmission-line theory can be used even in metal wires of rather small dimensions.

VII. DISCUSSION

Using a simple approach where the electrons are accelerated by the electromagnetic field they collectively cause, we have calculated the small signal propagation velocity in electron waveguides and found that it is very low compared to the velocity of light. Transmission-line equivalents have been given to visualize the scattering for the plasma waves at various junctions. One interesting consequence is the strong reflections at junctions between bulk conductors and electron waveguides. Another result concerns reflections at elastic scatterers. These reflections are shown to be unexpectedly small when the equivalent characteristic impedance of the plasma waveguide is high. This could reduce the ability to switch high-frequency signals in an electron waveguide device. It would also be interesting to calculate the effects of nonlinearities neglected in (13) and the dispersion present at higher frequencies to see what happens to short and intense pulses. Is there a space-charge soliton? Another direction of development for this work is to calculate scattering for plasma waves in general multiports. This would further help in the design of high-frequency electron waveguide devices.

ACKNOWLEDGMENTS

The author thanks Olle Nilsson, Thomas Palm, Lars Thylén, and Eilert Berglind for helpful discussions.

[1] S. Datta, Superlatt. Microstruct. **6**, 83 (1989).
[2] J. A. del Alamo and C. C. Eugster, Appl. Phys. Lett. **56**, 78 (1990).
[3] F. Sols, M. Macucci, U. Ravaioli, and K. Hess, J. Appl. Phys. **66**, 3892 (1989).
[4] T. Palm and L. Thylén, Appl. Phys. Lett. **60**, 237 (1992).
[5] T. Palm, L. Thylén, O. Nilsson, and C. Svensson, J. Appl. Phys. **74**, 687 (1993).
[6] T. J. Thornton, M. Pepper, H. Ahmed, D. Andrews, and G. J. Davies, Phys. Rev. Lett. **56**, 1198 (1986).
[7] M. Bonitz, R. Binder, D. C. Scott, S. W. Koch, and D. Kremp, Phys. Rev. E **49**, 5535 (1994).
[8] B. S. Mendoza and W. L. Schaich, Phys. Rev. B **43**, 6590 (1991).
[9] R. Bergmann, A. Menschig, G. Lehr, P. Kübler, J. Hommel, R. Rudeloff, B. Henle, F. Scholz, and H. Schweizer, J. Vac. Sci. Technol. B **10**, 2893 (1992).
[10] M. Büttiker, J. Phys. Condens. Matter **5**, 9361 (1993).
[11] M. Büttiker, Phys. Rev. Lett. **57**, 1761 (1986).
[12] M. Büttiker, IBM J. Res. Dev. **32**, 317 (1988).